34th Annual International Conference of the IEEE EMBS
San Diego, California USA, 28 August - 1 September, 2012

Parcellation of Human Inferior Parietal Lobule Based on Diffusion MRI

Bilge Soran[1] Zhiyong Xie[2] Rosalia Tungaraza[3] Su-In Lee[1] Linda Shapiro[1,2] Thomas Grabowski[3]

Abstract— **The function of a brain region can be constrained by its anatomical connections. The Inferior Parietal Lobule (IPL) is a cortical region with marked functional heterogeneity, involved in visuospatial attention, memory, language and mathematical cognition. In this work three different variants of the normalized graph-cut clustering algorithm were applied to obtain a parcellation of the IPL of living subjects into component regions based on the estimate of anatomical connectivity obtained from diffusion tensor tractography. Results over the three different algorithms were compared and a new metric proposed to measure the quality of individual parcellations by comparing to standard atlas regions. In this study of 19 subjects, an average of 64% overlap with the Juelich brain atlas was observed.**

I. INTRODUCTION

Diffusion MRI can be used to noninvasively study the anatomical structure of the brains of living subjects. Tractography algorithms have been developed that estimate anatomical connections from diffusion weighted MR images [1]. Parcellations based on these anatomical connections provide valuable information for exploring functional connectivity relationships. According to the gold standard of cytoartchitecture, the IPL consists of seven distinct functional fields. However, cytoartchitecture only works with postmortem brain samples. In this study the aim is to parcellate the IPL data of living subjects according to an anatomical connectivity map and evaluate the parcellation quality by means of the overlap with clusters of a standard atlas. The cortical area can be parcellated into distinct clusters based on the cross-correlation of the connectivity map estimated from diffusion MRI by probabilistic tractography. Current methods fall into three major categories. The first category relies on the known connection patterns of the functional fields. Either local information about the diffusion or the connectivity information derived from tractography can be applied. A second category uses a statistical model based on the assumption of the statistical distribution of the data [2]. Finally a third category uses unsupervised machine learning methods to cluster the voxels based on voxel-wise connectivity differences [3], [4], [5]. In this project the normalized graph-cut clustering algorithm, an unsupervised machine learning technique, was used to parcellate the IPL region.

This work was supported by NIH-NINDS Grant No. RC4-NS073008 (PI: T. Grabowski).

[1]Dept. of Computer Science and Engineering, University of Washington {bilge, suinlee, shapiro} at cs.washington.edu

[2]Dept. of Electrical Engineering, University of Washington zyxie at u.washington.edu

[3]Intergrated Brain Imaging Center, University of Washington {rltungar, tgrabow} at u.washington.edu

A substantial difficulty in *in vivo* brain parcellation is the lack of ground truth. The Juelich Atlas, which was used in this work, is an average map of the brain, obtained from 10 post-mortem subjects, and contains 7 IPL regions. The actual number of parcels in an IPL of a human being that can be obtained through diffusion MRI is still a subject of debate. Therefore, the evaluation of the quality of the parcellation is a problem. In this paper a new metric that can be used to evaluate the quality of a parcellation of a brain as compared to an atlas when there is no ground-truth for the individual brain is proposed. This metric was used to compare the results of three different clustering algorithms on 19 living subjects.

II. PREPROCESSING

Our data consisted of DWI (64 unique directions and b-value of 1000 mm/s2) with 2 mm isotropic resolution belonging to 19 healthy control subjects obtained through a Siemens Trio 3T scanner. We had diffusion, non-diffusion and T1-weighted MRI volumes for all subjects. After removing the noise and eddy current distortions from the raw data by applying affine registration of all volumes to a non-diffusion weighting volume, a 2mm white/grey matter boundary was extracted and the voxels along that boundary were used to define both the target regions and seed regions. The target regions came from all the 2009-Destrieux parcels provided by Freesurfer[6], and the seed regions were the voxels along the white/grey matter interface that belonged to either the left angular gyrus, the left supramarginal gyrus, or the left Jensen sulcus. Probabilistic tractography was performed on a voxel by voxel basis using Mrtrix[7]. During tractography all tracks that started and ended within the same ROI were rejected. The likehood of connection between IPL and non-IPL cortical areas was calculated by counting the number of tracts that reached each cortical target from 5000 particles that were initiated from each IPL voxel.

A. Data for Clustering

Our clustering data contains 3D coordinates of the IPL voxels and the target connectivity probabilities of each seed voxel obtained by probabilistic tractography in the preprocessing step. Target regions showing no connectivity with any seed voxels are discarded.

III. FEATURE SPACE

The form of the feature space is dependent on the clustering algorithm. In preliminary studies we determined that the normalized graph-cut family of algorithms produced more meaningful clusters and more repeatable results than

such standard algorithms as K-means and EM (Expectation-Maximization) clustering. For the normalized graph-cut algorithm, the feature space is a graph that must be partitioned into subsets. A weighted undirected graph G = (V, E) is constructed, where each node V represents a voxel and an edge is formed between every pair of nodes. The weight on each edge w_{ij} represents the strength of the similarity according to some metric between nodes i and j. This graph structure was used to construct a V*V composite similarity matrix W in which each W_{ij} represents the similarity of two voxels by means of *both* connectivity and spatial affinity. Fig.1 illustrates the construction of the composite similarity matrix; the steps are as follows:

1) Build a normalized connectivity matrix using probabilistic tractography. The values are normalized by dividing by the largest value of the matrix.
2) Build a symmetric spatial distance matrix according to the L_∞ metric:

$$dist(i,j) = max(|i_x - j_x|, |i_y - j_y|, |i_z - j_z|) \quad (1)$$

The values are normalized by dividing by the largest value of the matrix.
3) Compute a connectivity similarity matrix according to the equation:

$$W_{conn}^{i,j} = exp(-\alpha * f_{conn}(p_i, p_j)/\sigma_{conn}^2) \quad (2)$$

where f_{conn} is the Jaccard metric defined as [8]:

$$d_{st} = 1 - \frac{\#\left[(x_{sj} \neq x_{tj}) \cap ((x_{sj} \neq 0) \cup (x_{tj} \neq 0))\right]}{\#\left[(x_{sj} \neq 0) \cup (x_{tj} \neq 0)\right]} \quad (3)$$

where x_{sj} represents the connectivity of seed voxel s to target region j. Note that multiple other distances such as Euclidean and Mahalanobis distances were also tried, and Jaccard distance performed the best.
4) Compute a spatial affinity matrix with the equation below, proposed by Shi and Malik [9]:

$$W_{spatial}^{i,j} = exp(-(1-\alpha) * dist(i,j)/\sigma_{spatial}^2) \quad (4)$$

5) Compute the composite similarity matrix:

$$W_{similarity}^{i,j} = W_{conn}^{i,j} + W_{spatial}^{i,j} \quad (5)$$

where i, j represents the i^{th} and j^{th} voxels respectively and x, y, z represents the 3D coordinates. The parameter α controls the contribution of the connectivity matrix and spatial matrix to the similarity matrix, and σ is a weighting factor, used for similarity measurement. This method is similar to that in [9], but uses a linear combination of connectivity and spatial affinity instead of a product.

IV. PARCELLATION

The purpose of this project is to parcellate the voxels into disjoint sets $S_1, S_2, ..., S_m$ based on the connectivity and spatial affinity information represented by the composite similarity matrix. One such class of techniques suitable for this purpose is spectral clustering, which aims to perform dimensionality reduction by using the spectrum of the similarity matrix. Normalized graph cuts, first proposed by Shi and Malik [9], is in this class of algorithms and is commonly used for image segmentation. There are different approaches for normalized graph-cut clustering algorithms, and in this project we experimented with three of them: standard normalized graph cuts, normalized graph cuts with feature selection, and normalized graph cuts with K-means.

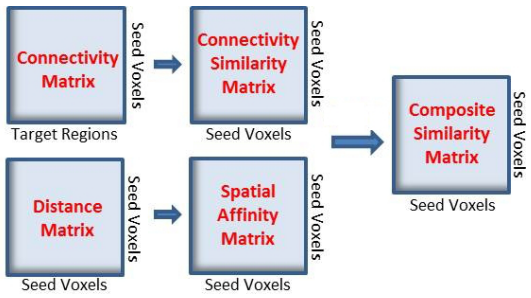

Fig. 1. Construction of Similarity Matrix

A. Standard Normalized Graph Cuts (NGC-std)

The standard normalized graph-cuts clustering algorithm represents the feature space as a graph. It partitions the vertices of the graph into two sets (S_1, S_2) based on the eigenvector v, corresponding to the second-smallest eigenvalue of the generalized eigenvalue problem. Let $d(i) = \sum_j w_{ij}$ be the total connection from node i to all other nodes, and let D be an N×N diagonal matrix with d on its diagonal. With W representing the undirected weighted graph as an N×N symmetrical composite similarity matrix with $W_{ij} = w_{ij}$, the equation

$$(D - W)y = \lambda Dy \quad (6)$$

represents the generalized eigenvalue problem. The details of composite similarity matrix computation were given in section 3, and the steps of the normalized graph-cuts algorithm are given below:

1) Given a feature space, set up a weighted graph G = (V, E), compute the weight on each edge, and summarize the information into W and D.
2) Solve $(D - W)y = \lambda Dy$ for eigenvectors with the smallest eigenvalues.
3) Use the eigenvector with the second smallest eigenvalue to bipartition the graph by finding the splitting point such that the parameter Ncut (see below) is minimized.
4) Decide if the current partition should be subdivided by checking the stability of the cut. If Ncut is below the prespecified value, recursively repartition the segmented parts.

The number of groups segmented by this method is controlled directly by the maximum allowed value of Ncut, the normalized cut value between two sets S_1 and S_2 defined by:

$$Ncut(S_1, S_2) = \frac{cut(S_1, S_2)}{assoc(S_1, V)} + \frac{cut(S_1, S_2)}{assoc(S_2, V)} \quad (7)$$

Here, $cut(S_1, S_2)$ represents the degree of dissimilarity between S_1 and S_2, and is defined as $cut(S_1, S_2) = \sum w_{ij}$, where $i \in S_1$ and $j \in S_2$. The association between S_k, k $\in \{1, 2\}$ and V is defined as $assoc(S_k, V) = \sum w_{ij}$, where $i \in S_k$ and $j \in$ V.

B. Normalized Graph Cuts with Feature Selection (NGC-fea)

Some of the target regions might have similar connectivity patterns for all voxels. Such target regions are not valuable for clustering, since they do not carry discriminative information for parcellation purposes. These kinds of target regions are detected from the variance of the connectivities of each target region. After computing the variance for each target region, a threshold of 0.001 is applied to select the targets with high variances, since they are expected to carry discriminative information.

C. Normalized Graph Cuts with K-means

Another normalized graph-cut clustering approach described in [10] was also investigated.

- Given a feature space, set up a weighted graph G = (V, E), compute the weight on each edge, and summarize the information into W and D.
- Solve $(D - W)y = \lambda Dy$ for the first k eigenvectors $v_1, v_2, .., v_k$.
- Build a matrix U with $v_1, v_2, .., v_k$ as columns. Use K-means to cluster the matrix U into $c_1, c_2, .., c_k$ clusters.

While the standard normalized graph-cuts algorithm can be unstable for cuts where similar Ncut values exist for different cutting positions, this approach can also exhibit unstable behaviour because of the random seed selection in the K-means algorithm.

V. EVALUATION METRIC

In this study, in order to measure the overlap between the Juelich atlas and the computed clusters, a new metric was designed. Fig. 2 shows an example table used in the evaluation. Here rows and columns of the table represents the computed clusters (CC) and the atlas clusters (AC), respectively. Each cell represents the number of intersecting voxels between a cluster of the atlas and a normalized cut cluster.

	AC 1	AC 2	AC 3	AC 4	AC 5	AC 6	AC 7
CC 1	0	0	0	91	15	3	0
CC 2	0	0	0	24	0	79	8
CC 3	0	53	67	9	0	0	0
CC 4	6	78	14	4	0	0	2
CC 5	91	31	0	0	0	0	0

Fig. 2. An example table used in evaluation.

For rows representing the computed clusters, columns representing the atlas clusters, and cells representing the number of intersecting voxels between a cluster of the atlas and a computed cluster of the subject brain, the metric R is defined as follows:
Let the normalized maximal scoring atlas cluster sum be given by:

$$A_{sum} = (\sum_i max(row_i))/(\sum_{ij} cell_{ij}) \quad (8)$$

A_{sum} is the sum of the largest overlap with the computed clusters of each atlas cluster. Let the normalized maximal scoring computed cluster sum be given by:

$$C_{sum} = (\sum_j max(column_i))/(\sum_{ij} cell_{ij}) \quad (9)$$

C_{sum} is the sum of the largest overlap with the atlas clusters of each computed cluster. Then, the metric R is given by:

$$R = \frac{A_{sum} + C_{sum}}{2} \quad if\ abs(A_{sum} - C_{sum}) < T \quad (10)$$

where T is an experimentally determined threshold and set to 0.2. The metric R considers both which computed cluster is assigned to which atlas cluster and which atlas cluster is assigned to which computed cluster. If the absolute difference between A_{sum} and C_{sum} is not less than the threshold, the resulting parcellation is unacceptable. In the ideal case, where the number of atlas clusters and computed clusters are the same, and each atlas cluster has the maximal overlap with a different one of the computed clusters, R becomes 1; meaning the computed clusters perfectly overlap with the atlas clusters. In the worst case, where there is only one computed cluster (no clustering), C_{sum} becomes equal to 1, and A_{sum} becomes $L\ /(\sum_{ij} cell_{ij})$, where L is the size of the largest atlas cluster. Because of the distribution of the voxels into atlas clusters, the value of A_{sum} is about .30, making the difference between A_{sum} and C_{sum} $(1 - .30)$ larger than the threshold, meaning an unacceptable parcellation.

VI. EXPERIMENTS AND RESULTS

The data set consisted of the left and right IPL regions, which have similar connectivity patterns [11], of 19 subjects. The right IPL data set was divided into two with 10 subjects for training and 9 for testing; the left IPL data set was used only for testing. This resulted in 10 subjects for training and 28 subjects for testing. The three different normalized cut algorithms were run on the training set, and the best parameter set for each algorithm was selected by looking at the average overlap of the atlas and the subjects in the training set. Because the Juelich atlas contains 7 manually determined clusters, experiments were run with +/- 2 margin of 7, namely 5 to 9 clusters and with α varying from 0.5 to 0.9 with 0.1 intervals. The normalized graph cuts with K-means approach did not produce any acceptable parcellation results according to the proposed metric.

After the best parameters were determined on the training set, both algorithms were run on the whole training and testing sets. Fig. 4 shows the parcellation performances. The training set is marked in yellow. Though 7 clusters are represented in the atlas, 5 clusters gave the best result of

.64 while 7 clusters gave a result of .61. A Kolmogorov-Smirnov test showed that the difference between these results are statistically significant. Furthermore, Mars *et al.* in [4] obtained 5 clusters in their 2011 study. Whether the discrepancy is due to technical limitations (in MRI acquisition, diffusion imaging post-processing or clustering approaches) or to differences between parcels as defined by cytoarchitecture versus connectivity will be the focus of further work. Improvements in technical approach can be tracked by metrics such as the one proposed here.

Subject	Right Hemisphere		Left Hemisphere	
	NGC-std	NGC-fea	NGC-std	NGC-fea
1	0.625392	0.626959	0.615437	0.620902
2	0.753577	0.751987	0.609091	0.610909
3	0.718487	0.710084	0.604126	0.608055
4	0.569952	0.570747	0.672694	0.674503
5	0.652021	0.655536	0.675652	0.672174
6	0.637883	0.646240	0.706388	0.707617
7	0.640599	0.640599	0.553792	0.554674
8	0.593415	0.601072	0.592657	0.599650
9	0.627622	0.628497	0.636494	0.635057
10	0.683212	0.682482	0.566836	0.564298
11	0.590669	0.590669	0.627559	0.633071
12	0.611452	0.615542	0.640625	0.637336
13	0.747917	0.746875	0.620948	0.622195
14	0.657725	0.653433	0.691321	0.683432
15	0.666667	0.666667	0.592619	0.592619
16	0.657588	0.701362	0.660417	0.658333
17	0.600768	0.599808	0.642747	0.642747
18	0.611494	0.611494	0.716960	0.712555
19	0.670802	0.669847	0.644431	0.643819
AVERAGE	0.648276	0.651047	0.635305	0.635471

Fig. 3. Parcellation performances. The yellow area is the training data and the grey area is the independent test set.

To better illustrate the results, the parcellations for the left IPL of subjects 6, 14 and 18 are shown with the Juelich Atlas in Fig. 5. This figure shows only gray matter-white matter interface voxels. The computed clusters were colored according to the closest atlas cluster color in terms of distance between centers of gravity.

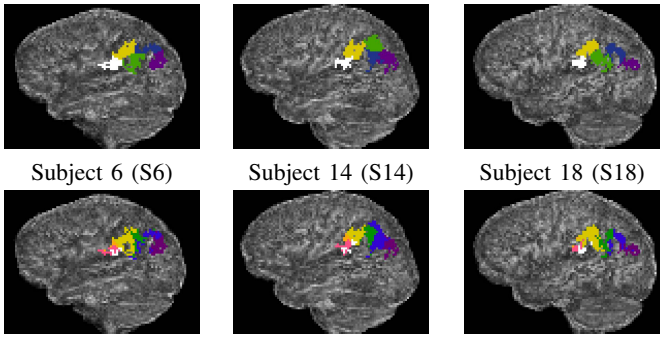

Subject 6 (S6) Subject 14 (S14) Subject 18 (S18)

Juelich Atlas in S6 diffusion space | Juelich Atlas in S14 diffusion space | Juelich Atlas in S18 diffusion space

Fig. 4. Juelich atlas and parcellation results in sagittal view

VII. Conclusion and Future Work

The function of a brain region can be constrained by its anatomical connections. The IPL is the cortical region whose different sub-regions represent different connection patterns. The importance of this work is in its investigation of methods for parcellating the IPL region of a living subject, rather than manual parcellation of a post-mortem subject. The output of such a parcellation can be very useful for future research in understanding human brain functionality. The main difficulty of such an evaluation is the lack of ground truth data by which to measure the quality of the parcellation. The ground-truth data available for this study was the Juelich atlas, which is an average brain map of 10 post-mortem subjects. Since it is only an average, perfect overlap with individual subjects is not possible. Individual subjects' brains might have different sizes for regions with different functionalities. Even if the 3D volume of the subject and the atlas overlap perfectly, the size of the regions might be different.

The main contributions of this work are the thorough study of clustering methods and parameters and the development of a new evaluation metric to measure the overlap between a parcellation and an atlas. This metric can be used with any kind of atlas, even if there is no individual ground-truth. One of its best properties is that it works with different numbers of clusters and detects if a parcellation is not of sufficient quality to be useful. This is only an initial study. Future plans include increasing the experiment space and using more sophisticated statistical analysis methods for parameter optimization. Different preprocessing and clustering approaches will be tried, and additional feature generation and selection methods will be applied.

References

[1] P. G. P. Nucifora, et al. Diffusion-Tensor MR Imaging and Tractography: Exploring Brain Microstructure and Connectivity. *Radiology*, 245(2):367–384, 2007.

[2] S. Jbabdi and M. W. Woolrich and T. E. Behrens. Multiple-subjects connectivity-based parcellation using hierarchical Dirichlet process mixture models. *NeuroImage*, 44(2):373–384, 2009.

[3] A. Anwander, et al. Connectivity-Based Parcellation of Broca's Area. *Cereb. Cortex*, 17(4):816–825, 2007.

[4] R. B. Mars, et al. Diffusion-Weighted Imaging Tractography-Based Parcellation of the Human Parietal Cortex and Comparison with Human and Macaque Resting-State Functional Connectivity. *The Journal of Neuroscience*, 2011.

[5] M. Ruschel, et al. Connectivity-based parcellation of the human inferior parietal cortex - New insights into the problem of structure-function relationships in humans and macaques, 2009.

[6] B. Fischl, M. I. Sereno, and A. Dale. Cortical surface-based analysis: II: Inflation, flattening, and a surface-based coordinate system. *NeuroImage*, 9(2):195 – 207, 1999.

[7] J-D. Tournier, F. Calamante, and A. Connelly. Robust determination of the fibre orientation distribution in diffusion mri: Non-negativity constrained super-resolved spherical deconvolution. *NeuroImage*, 35(4):1459 – 1472, 2007.

[8] MathWorks. `http://www.mathworks.com/help/toolbox/stats/pdist.html`, 2011.

[9] J. Shi and J. Malik. Normalized Cuts and Image Segmentation. *IEEE Transactions on Pattern Analysis and Machine Intelligence*, 22(8):888–905, 2000.

[10] U. von Luxburg. A tutorial on spectral clustering. Technical Report 149, Max Planck Institute for Biological Cybernetics, 2006.

[11] S. Caspers, et al. Probabilistic fibre tract analysis of cytoarchitectonically defined human inferior parietal lobule areas reveals similarities to macaques. *NeuroImage*, 2011.